

# Sonochemical Synthesis of $\text{SrBaFe}_x\text{Mo}_{2-x}\text{O}_6$ ( $x=1.0, 1.1, 1.3$ and $1.4$ ) Double Perovskites: Characterization and Magnetic Properties

S. Varaprasad<sup>1,\*</sup>, K. Thyagarajan<sup>2</sup>

<sup>1</sup>Department of Physics, Jawaharlal Nehru Technological University, Ananthapuramu, Andhra Pradesh, India

<sup>2</sup>Department of Physics, Jawaharlal Nehru Technological University Anantapur College of Engineering, Pulivendul, YSR District, Andhra Pradesh, India

## Abstract

This work investigates ultrasound assisted synthesis, characterization and magnetic properties of  $\text{SrBaFe}_x\text{Mo}_{2-x}\text{O}_6$  ( $x=1.0, 1.1, 1.3$  and  $1.4$ ) double perovskites. X-ray diffraction (XRD) analysis confirmed proposed that samples are in single phase. It was found that lattice constants decrease with increase in composition  $x$ . Morphology of all samples was examined by Scanning Electron Microscopy (SEM) images. Energy Dispersive X-ray Spectroscopy (EDS) data confirmed purity and nonexistence of foreign elements in prepared samples. Fourier transform infrared spectroscopy (FTIR) studies revealed formation of perovskite structure. It was noticed that Fe-Mo degree of ordering decreases with an increase in composition  $x$ . Saturation magnetization of prepared samples decreased with increase of composition  $x$ , which is correlated with Fe-Mo degree of ordering.

**Keywords:** Double perovskite, sonochemical, characterization, magnetic properties

\*Author for Correspondence E-mail: svpphy2@gmail.com

## INTRODUCTION

Double perovskite structure of general formula  $\text{A}_2\text{BB}'\text{O}_6$  (A= alkali earths and B, B' = transition metals) with half-metallic nature have drawn great interest due to use in magnetoresistance and spintronic applications. Diversified applications because of high spin polarization, soft magnetic nature and high Curie temperature of these Fe-Mo based double perovskite, have attracted researchers worldwide [1–3]. Double perovskite crystal structure consists of alternating  $\text{BO}_6$  and  $\text{B}'\text{O}_6$  octahedra in the lattice [4–8]. The magnetic structure of  $\text{A}_2\text{FeMoO}_6$  consists of ordered arrangement of parallel  $\text{Fe}^{3+}$  ( $3d^5$ ,  $s=5/2$ ) magnetic moments, antiferromagnetically coupled with  $\text{Mo}^{5+}$  ( $4d^1$ ,  $s=1/2$ ) spins.  $\text{A}_2\text{FeMoO}_6$  magnetic properties are mostly influenced by anti-site disorder at B & B' sites leading to a reduction in magnetic saturation ( $M_s$ ) of  $\text{Sr}_2\text{FeMoO}_6$  material. Therefore, it is beneficial to study the correlation between degree of Fe/Mo ordering, magnetic properties and magnetoresistance on  $\text{A}_2\text{FeMoO}_6$  (A=Sr,

Ba, Ca and SrBa) [9–17]. Many investigations have already reported on correlation between magnetic structure, degree of ordering and magnetoresistance of systems like  $\text{Sr}_2\text{Fe}_x\text{Mo}_{2-x}\text{O}_6$  and  $\text{Sr}_2\text{Fe}_{1-x}\text{Mo}_{1-x}\text{O}_6$  at different compositions of  $x$  [18–22]. It is observed from the literature that degree of ordering and magnetoresistance are optimum at  $x=1$  and then decreases as  $x$  deviates. It has been reported recently that  $\text{SrBaFeMoO}_6$  system shows a systematic decrease in  $T_c$  and increase in  $M_s$  with maximum Low Field Magnetoresistance (LFMR). An extensive study of  $\text{A}_2\text{FeMoO}_6$  (A=Sr, Ba, Ca and SrBa) has been carried out using different synthesis methodologies but no literature has been reported on sonochemical methodology for double perovskite system so far; even though extensive studies on single perovskite of  $\text{ABO}_3$  system have been done using sonochemical method [23–28]. The sonochemical method is very promising in preparing powders at relatively low preparation temperature ( $950^\circ\text{C}$ ) under the influence of the ultrasonic waves [29–30].

In view of this, in the present study, authors tried to adopt sonochemical chemical method for its advantage over other methodologies to investigate  $SrBaFe_xMo_{2-x}O_6$  ( $x=1.0, 1.1, 1.3$  and  $1.4$ ) double perovskites. The samples under study were characterized by XRD, SEM, EDS, FTIR and VSM.

## EXPERIMENTAL WORK

Polycrystalline samples of  $SrBaFe_xMo_{2-x}O_6$  ( $x=1.0, 1.1, 1.3$  and  $1.4$ ) (SBFMO) were synthesized by sonochemical method. Exact proportional amounts of analytical grade chemicals such as  $Sr(NO_3)_3$ ,  $Ba(NO_3)_3$ ,  $Fe(NO_3)_2 \cdot 9H_2O$  and  $H_2MoO_4$  were added in a beaker of 200 ml double distilled water and stirred on magnetic stirrer at room temperature (RT) until clear solution is formed, to this citric acid is added in 2:1 mole ratio (citric acid to metal ion), solution is again stirred for 10 min to obtain clear solution. A highly intense sonication of frequency 20 kHz was carried out with a horn made up of titanium at a temperature of 353 K (Sonics-Vibra cell, USA) for about 20 min. After sonication, ammonia is added to the solution to adjust pH to  $\sim 7$ . Solution is kept on a hot plate of a magnetic stirrer at  $80^\circ C$  and ethylene glycol is added in 1:1.2 ratio (metal ion to ethylene glycol). The resulting solution is kept in a hot air oven at  $230^\circ C$  for 24 h, the residue formed was collected and dried on Bunsen burner at  $250^\circ C$  for about 5 min to obtain a required composition and further ground to get homogenous powder.

The resulting powders were taken into crucibles and made to undergo heat treatment at 400, 600 and  $800^\circ C/6$  h with intermittent grounding. The obtained powders were pressed into pellets of 1 cm diameter and 2 mm thickness using a die by applying 2 tons/ $m^2$ . The resulting pellets were sintered at  $950^\circ C$  for 6 h. For reducing the  $Mo^{6+}$  to  $Mo^{5+}$  or loss

of oxygen, the pellets were heated at  $950^\circ C$  in a stream mixture of 10%  $H_2/Ar$  gas for about 6 h.

The final materials are subjected to X-ray diffraction (Philips PW-1830) studies to confirm the structure. SEM (Zeiss INCA) studies are done to confirm the grain size, EDS (Oxford INCA EDX) is carried out on all samples to check purity and elements present. FTIR (PerkinElmer spectrum two) spectra are used to analyze all samples to confirm perovskite formation. Magnetic measurements were done on SBFMO compound using VSM (EZ9, Microsense Inc, USA) at applied magnetic field from  $-20$  to  $+20$  kOe.

## RESULTS AND DISCUSSION

### Crystal Structures

The purity of phases of all SBFMO samples is shown in Figure 1. Compound was found to crystallize in cubic structure with space group  $Fm\bar{3}m$  as per X-ray diffraction patterns which are in excellent accord with reported literature [31]. Lattice parameters 'a' and unit cell volume 'V' were evaluated from indexed (hkl) values (220), (222), (400), (422), (440) and (620) and tabulated in Table 1. It is observed from Figure 2 that with an increase in Fe composition x, lattice parameters and unit cell volume decrease, reasons for deviation of lattice parameter are valence disproportion and the difference in radii of  $Fe^{3+}$  and  $Mo^{5+}$  [32, 33] of SBFMO compound, which is in accordance with Vegard's law [34].

### Scanning Electron Microscopy

Sintered pellets of  $SrBaFe_xMo_{2-x}O_6$  ( $x=1.0, 1.1, 1.3$ , and  $1.4$ ) were characterized to find grain size parameter using Scanning Electron Microscopy (SEM) and resulting micrographs are shown in Figure 3 (a-d). It is found that grain boundaries are clearly seen with grain size.

**Table 1:** Lattice Parameters (a) and Unit Cell Volume (V) of  $SrBaFe_xMo_{2-x}O_6$  ( $x=1.0, 1.1, 1.3$ , and  $1.4$ ).

Composition (x)	Space Group	a(Å)	V(Å) <sup>3</sup>
1.0	$Fm\bar{3}m$	7.9920	510.482
1.1	$Fm\bar{3}m$	7.9785	507.884
1.3	$Fm\bar{3}m$	7.9378	500.167
1.4	$Fm\bar{3}m$	7.9327	499.194

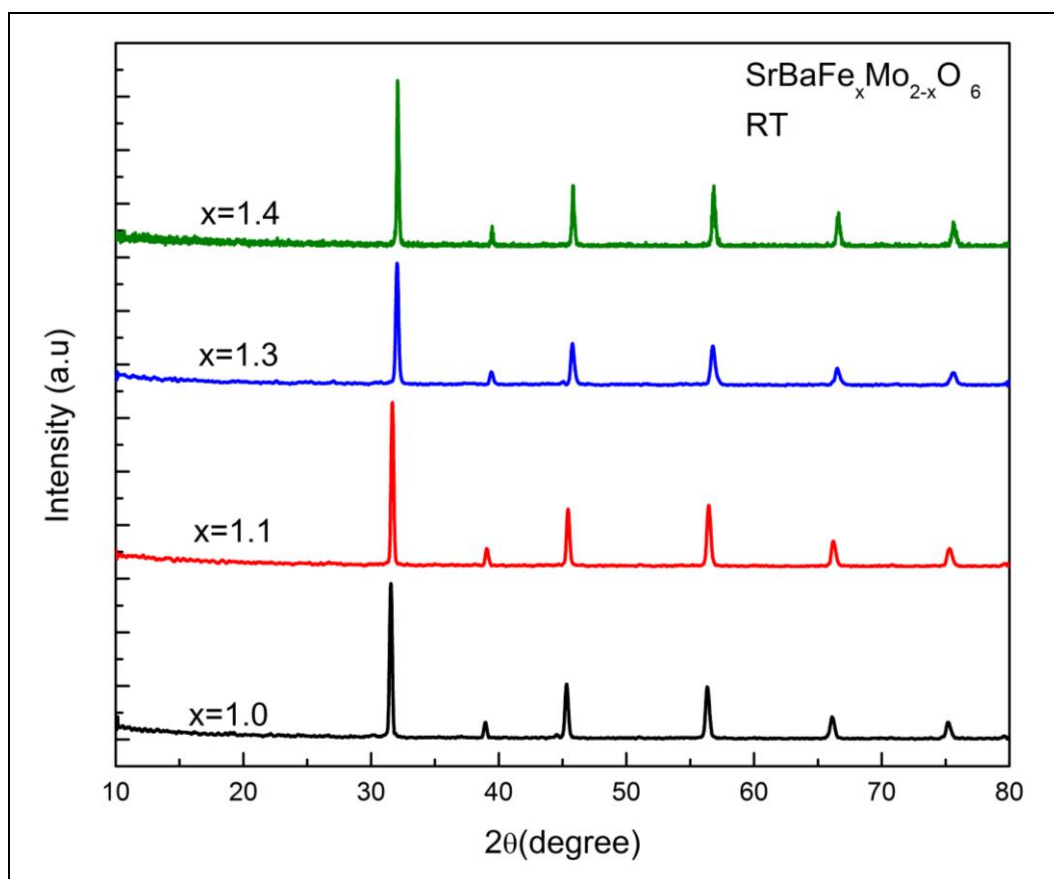


Fig. 1: X-Ray Diffraction Patterns for SBFMO.

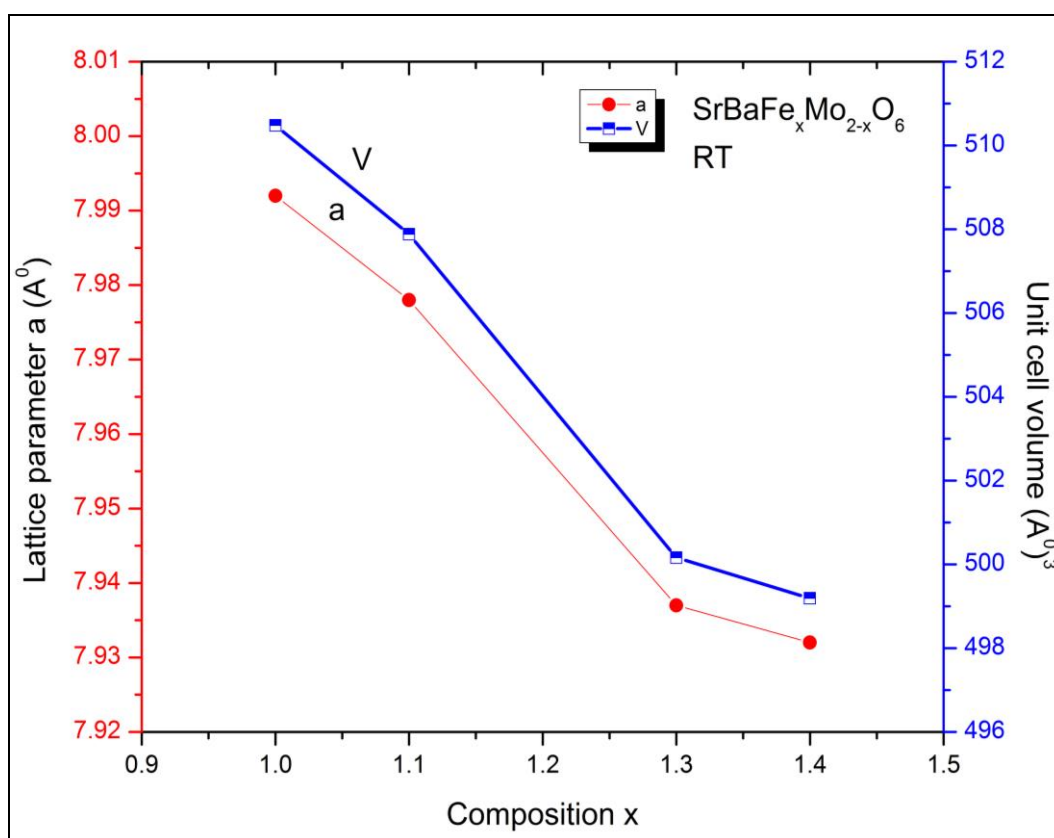
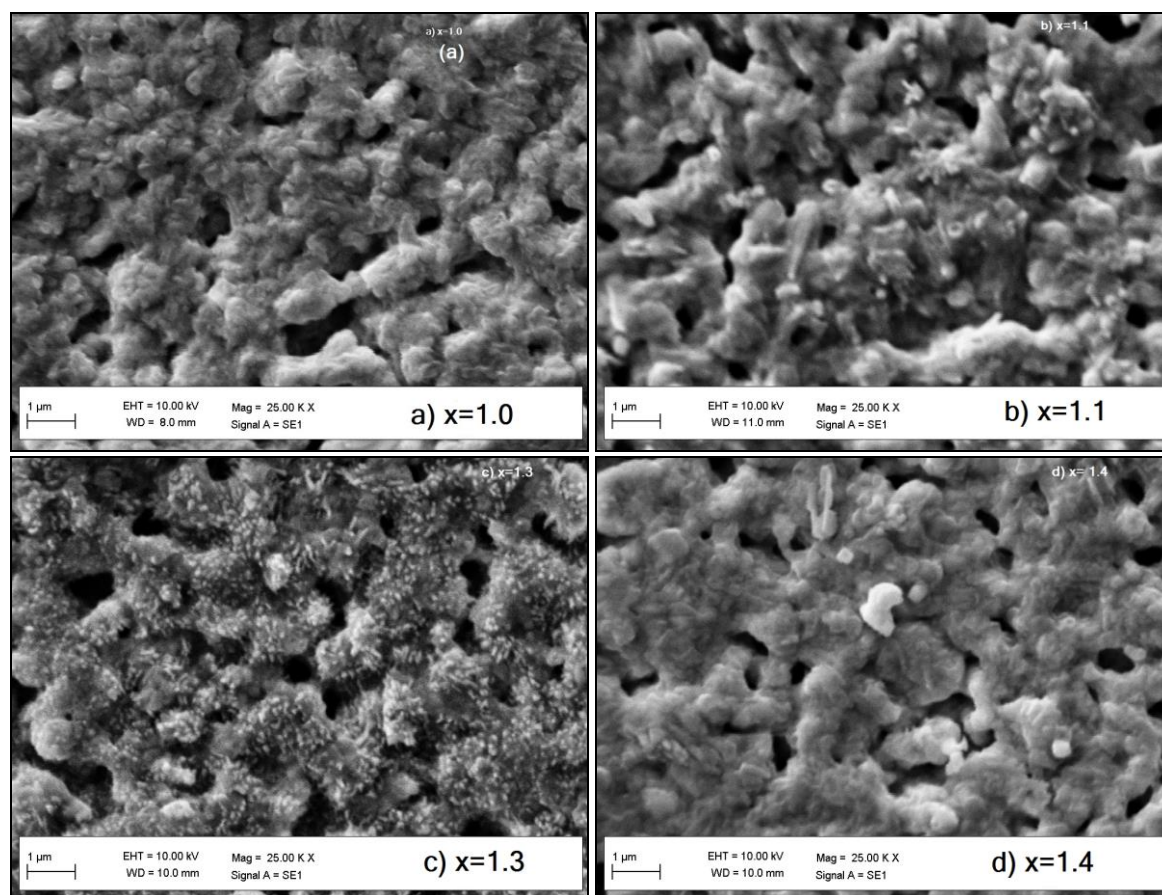


Fig. 2: Lattice Constants vs. Composition (x) for SBFMO.



**Fig. 3:** (a–d) Scanning Electron Microscopy Photographs of  $\text{SrBaFe}_x\text{Mo}_{2-x}\text{O}_6$  Samples for Composition: (a)  $x=1.0$ , (b)  $x=1.1$ , (c)  $x=1.3$  and (d)  $x=1.4$ .

### Energy Dispersive X-Ray Spectroscopy

Elemental data analyses for all samples of SBFMO compound were carried out to check the elements present and purity of the compound. Figure 4(a–d) shows the EDS spectra of  $\text{SrBaFe}_x\text{Mo}_{2-x}\text{O}_6$  ( $x=1.0, 1.1, 1.3$ , and  $1.4$ ). From EDS spectra, it is confirmed that all required or raw preparation composition elements (Sr, Ba, Fe, Mo and O) were present and no other elements (foreign/impurities) are existing.

### Fourier Transform Infrared Spectroscopy

Figure 5 shows FTIR spectra of the SBFMO samples in the spectral wave number range  $1000\text{--}400\text{ cm}^{-1}$  at room temperature. To confirm the perovskite phase formation, the FTIR spectra should have three characteristic absorption bands between  $850$  and  $400\text{ cm}^{-1}$  with respect to composition [35]. From Figure 5, FTIR spectra of the SBFMO samples under investigation detected bands for Fe and Mo, i.e., one strong band in the high wavenumber range ( $\sim 857.91\text{ cm}^{-1}$ ) associated to the Mo-O symmetric stretching mode of

$\text{MoO}_6$ -octahedra, another band at  $\sim 674.30\text{ cm}^{-1}$  assigned to the antisymmetric stretching mode of the  $\text{MoO}_6$ -octahedra, due to the higher charge of this cation [36]. A weak absorption band at about  $476.75\text{ cm}^{-1}$  is ascribed to Fe-O vibration absorption of  $\text{FeO}_6$ -octahedra.

### Atomic Ordering

In a unit cell, degree of ordering is study of favorable occupation of different atoms in respective sites [14]. For a solid solution  $\text{Mo}_{2-x}\text{Fe}_x$ , order of phase of is MoFe. The degree of ordering  $\eta$  can be calculated as:  $\eta = P_{\text{Mo}}^{(1)} - P_{\text{Mo}}^{(2)} = P_{\text{Fe}}^{(2)} - P_{\text{Fe}}^{(1)}$ , where  $P_{\text{Mo}}^{(1)}$ ,  $P_{\text{Mo}}^{(2)}$ ,  $P_{\text{Fe}}^{(1)}$  and  $P_{\text{Fe}}^{(2)}$  are relative occupancies of Mo and Fe atoms on Mo site and Fe site respectively, i.e.,  $P_{\text{Mo}}^{(1)} + P_{\text{Fe}}^{(1)} = 1$  and  $P_{\text{Mo}}^{(2)} + P_{\text{Fe}}^{(2)} = 1$ . Therefore, when complete disorder occurs,  $P_{\text{Mo}}^{(1)} = P_{\text{Mo}}^{(2)} = 1 - x/2$ ,  $P_{\text{Fe}}^{(1)} = P_{\text{Fe}}^{(2)} = x/2$ , and  $\eta = 0$ . When the maximum ordering is achieved,  $P_{\text{Mo}}^{(1)} = 1$ ,  $P_{\text{Mo}}^{(2)} = 1 - x$ ,  $P_{\text{Fe}}^{(1)} = 0$ ,  $P_{\text{Fe}}^{(2)} = x$ , and  $\eta_{\text{max}} = x$  for Mo-rich compounds ( $x \leq 1$ ), and  $P_{\text{Fe}}^{(2)} = 1$ ,  $P_{\text{Fe}}^{(1)} = x - 1$ ,  $P_{\text{Mo}}^{(2)} = 0$ ,  $P_{\text{Mo}}^{(1)} = 2 - x$ , and  $\eta_{\text{max}} = 2 - x$  for Fe-rich compounds ( $x \geq 1$ ).

In the present case, A is SrBa, B is Fe and B' is Mo in double perovskite  $A_2B_xB'_{2-x}O_6$ , Fe and Mo alternatively occupy the B and B' sites respectively. For B-rich compounds ( $x \geq 1.0$ ), maximum degree ( $\eta_{max}$ ) is  $2-x$  and for B'-rich compounds ( $x \leq 1.0$ ), maximum degree is  $x$  in  $SrBaFe_xMo_{2-x}O_6$  (i.e.  $A_2B_xB'_{2-x}O_6$ ) compounds and values are tabulated in Table 2. Plot showing maximum degree ( $\eta_{max}$ ) as function of composition is shown in Figure 6. It found from figure that the degree of the B/B'-site ordering is maximum at  $x=1.0$  and deviates (decreases at  $x=1.1, 1.3$ , and  $1.4$ ) from there on in  $SrBaFe_xMo_{2-x}O_6$  ( $x=1.0, 1.1, 1.3$  and  $1.4$ ) compound.

### Magnetization Measurements

Figure 7 shows magnetization versus applied magnetic field graph of  $SrBaFe_xMo_{2-x}O_6$  samples ( $x=1.0, 1.1, 1.3$  and  $1.4$ ) recorded at room temperature. Magnetic properties like saturation magnetization ( $M_s$ ), remanent magnetization ( $M_r$ ) and coercivity ( $H_c$ ) for BSFMO series have been obtained from Figure 7 and tabulated in Table 3. The variations of saturation magnetization ( $M_s$ ) with Fe composition ( $x$ ) of BSFMO compound are plotted in Figure 8. It is evident from Figure 8 that saturation magnetization was found to be maximum at  $x=1.0$  compared to

other compositions. The values of saturation magnetization were found to be 8.40 7.03, 4.95 and 4.54 e.m.u/g for  $x=1.0, 1.1, 1.3$ , and  $1.4$  respectively. This type of trend for saturation magnetization with Fe composition ( $x$ ) was correlated with degree of Fe/Mo ordering for  $Sr_2Fe_xMo_{2-x}O_6$  have been reported [37, 38], Mis-site (Fe-Mo) imperfection, oxygen deficiency and valence disproportion were quoted as reason [39]. From Figure 9, it is confirmed that correlation exists between degree of ordering and magnetic properties of BSFMO compound.

**Table 2:** Maximum Degree of Ordering ( $\eta_{max}$ ) of  $SrBaFe_xMo_{2-x}O_6$  ( $x=1.0, 1.1, 1.3$  and  $1.4$ ) System.

Composition (x)	Maximum Degree of Ordering ( $\eta_{max}$ )
1.0	1.0
1.1	0.9
1.3	0.7
1.4	0.6

**Table 3:** Magnetic Properties of  $SrBaFe_xMo_{2-x}O_6$  ( $x=1.0, 1.1, 1.3$  and  $1.4$ ) Double Perovskite.

Composition (x)	$M_s$ (emu/g)	$H_c$ (kOe)	$M_r$ (emu/g)
1.0	8.409	62.98	0.39
1.1	7.039	88.91	0.41
1.3	4.958	111.5	0.20
1.4	4.544	94.42	0.12

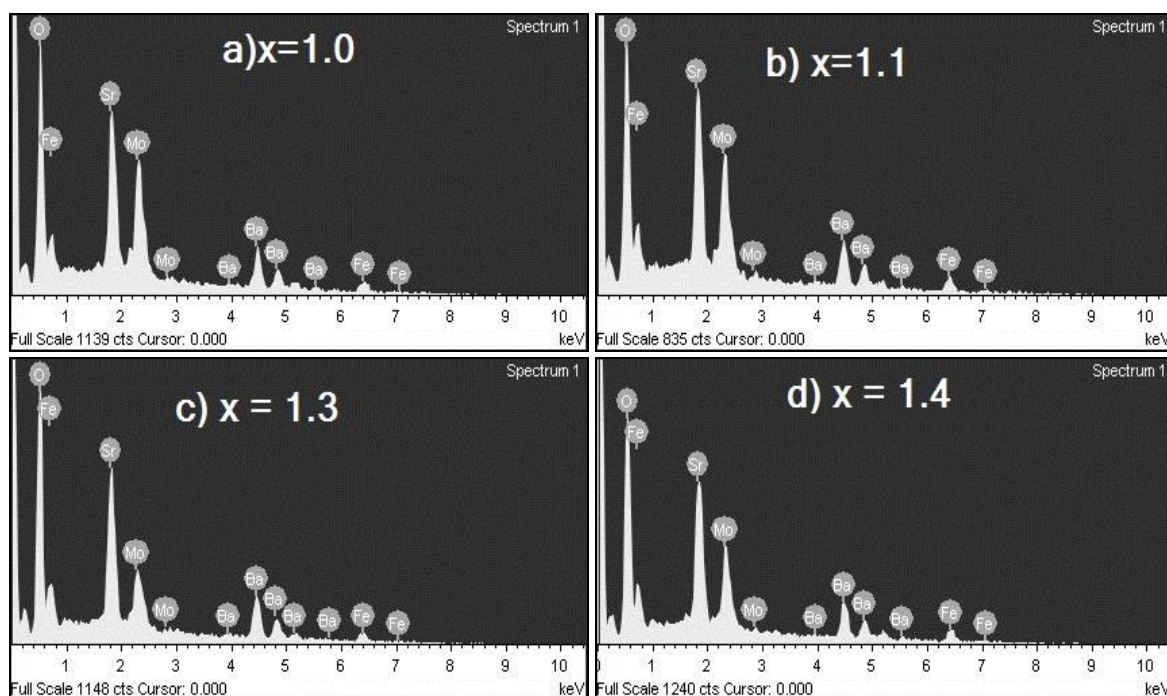


**Fig. 4:** (a–d) Energy Dispersive X-Ray Absorption Spectrographs of  $SrBaFe_xMo_{2-x}O_6$  Samples for Composition (a)  $x=1.0$ , (b)  $x=1.1$ , (c)  $x=1.3$  and (d)  $x=1.4$ .

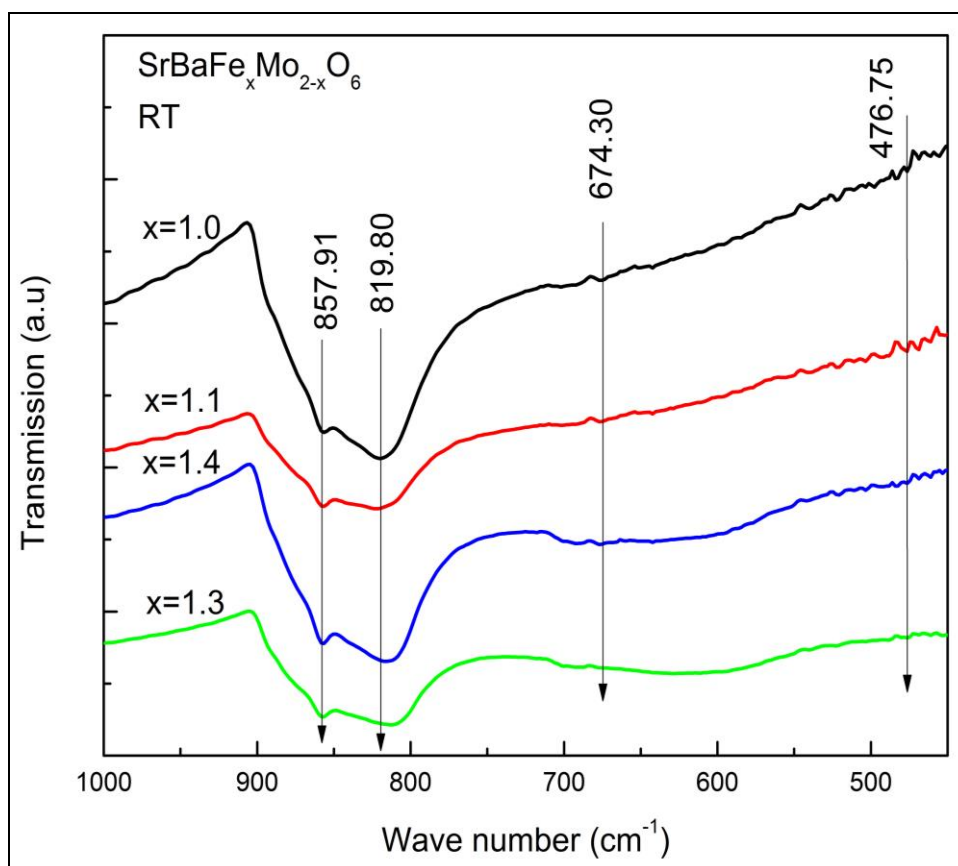


Fig. 5: Fourier Transform Infrared Spectroscopy of  $\text{SrBaFe}_x\text{Mo}_{2-x}\text{O}_6$  ( $x=1.0, 1.1, 1.3$  and  $1.4$ ).

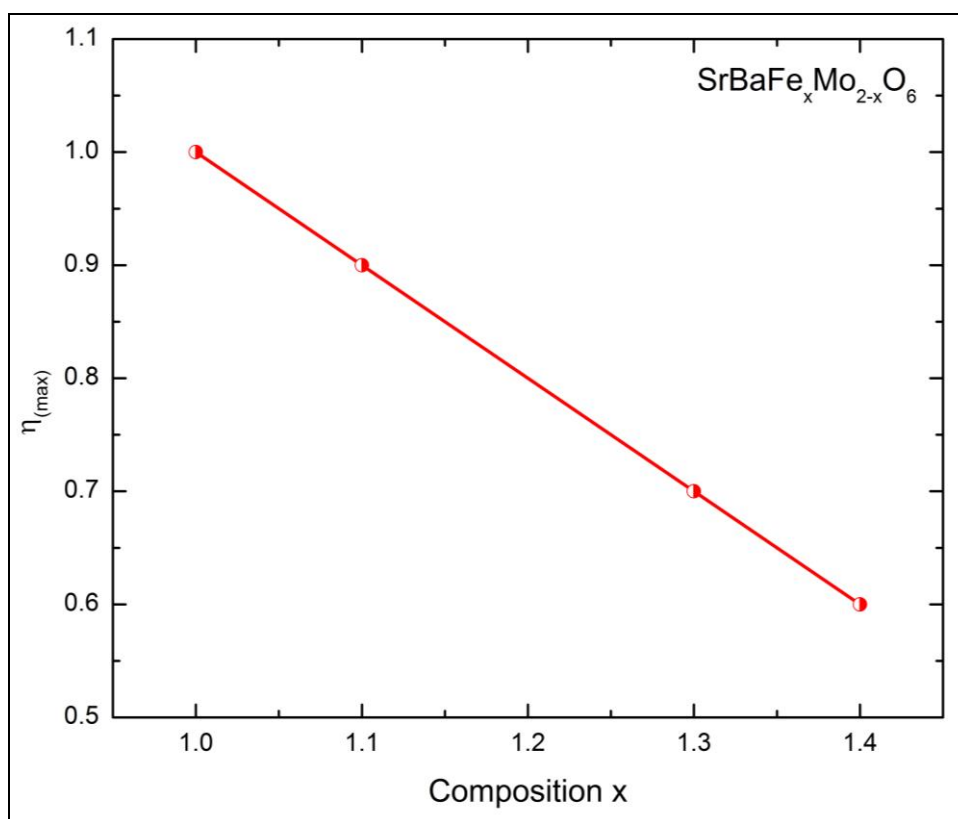


Fig. 6: Degree of Ordering as a Function of Composition  $x$  of  $\text{SrBaFe}_x\text{Mo}_{2-x}\text{O}_6$  ( $x=1.0, 1.1, 1.3$  and  $1.4$ ).

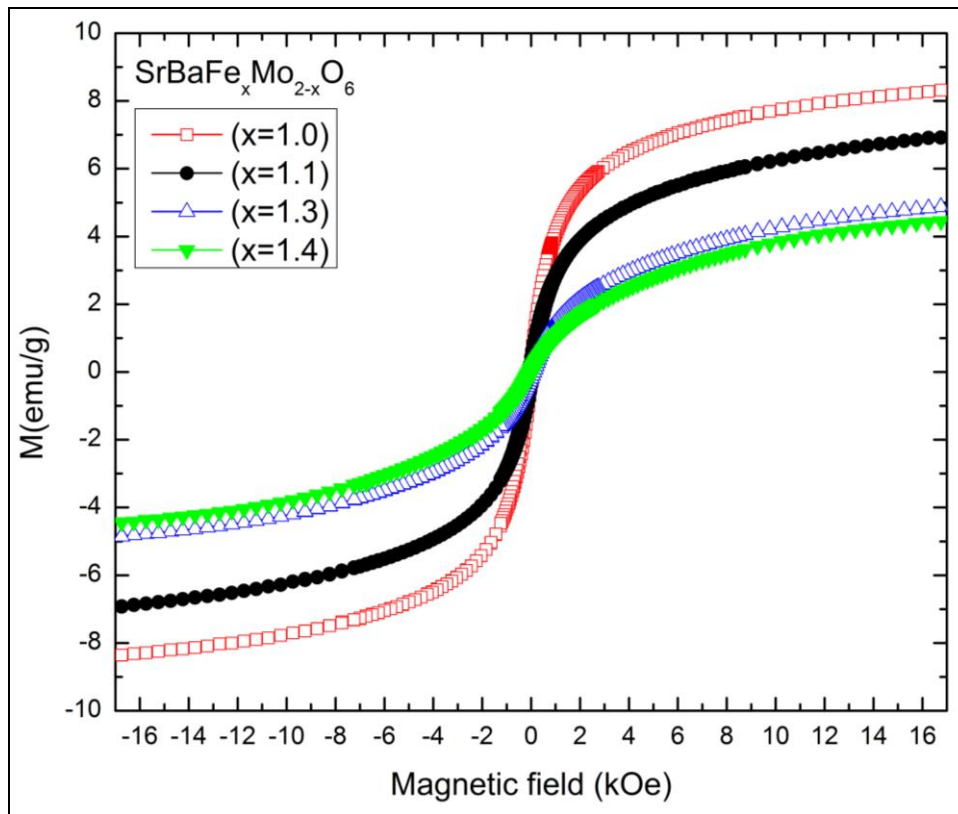


Fig. 7: Magnetic Field-Dependent Magnetization ( $M$ - $H$ ) Curves of  $\text{SrBaFe}_x\text{Mo}_{2-x}\text{O}_6$  Samples for Composition ( $x=1.0, 1.1, 1.3$  and  $1.4$ ).

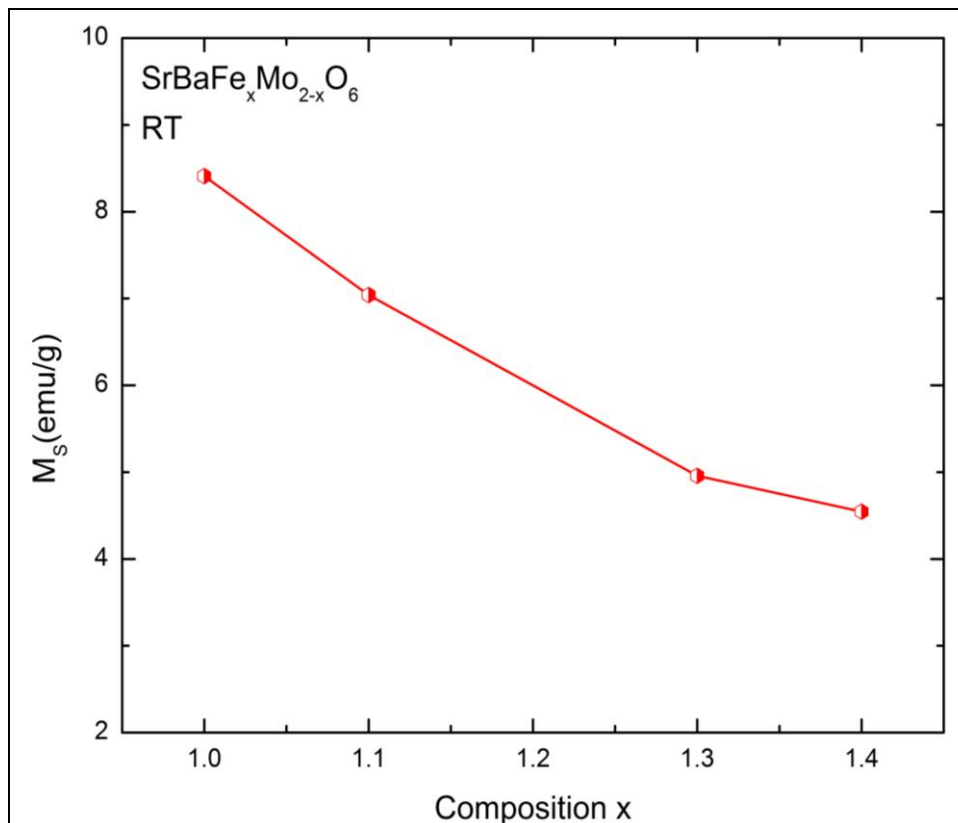
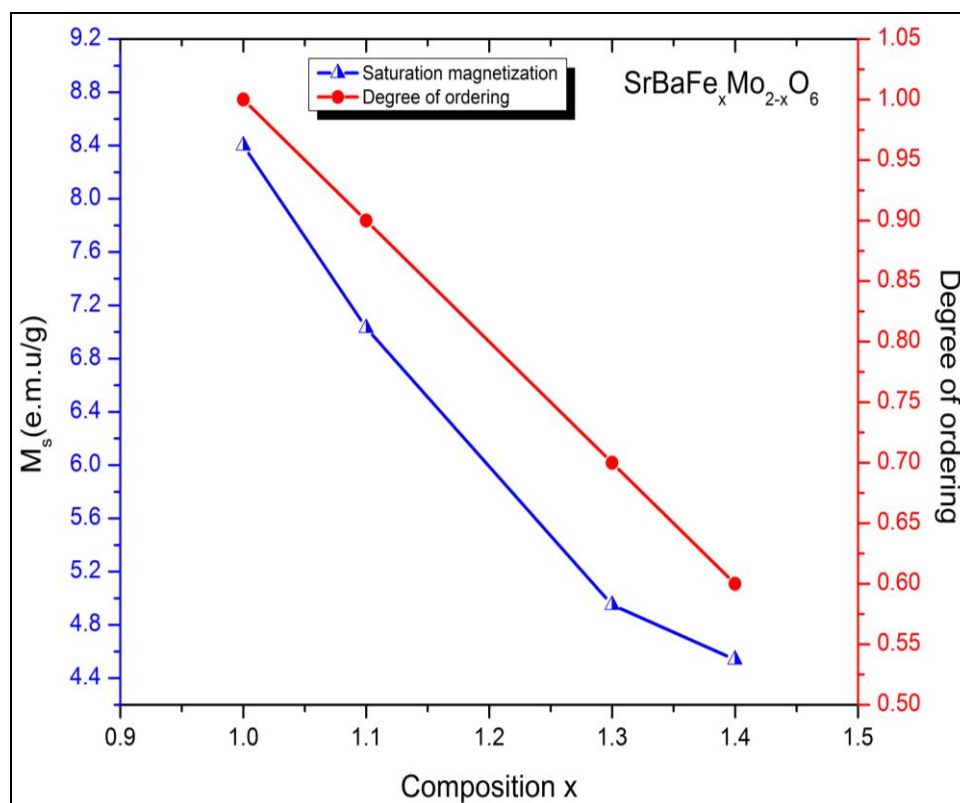


Fig. 8: Saturation Magnetization ( $M_s$ ) Dependence on Composition  $x$  of  $\text{SrBaFe}_x\text{Mo}_{2-x}\text{O}_6$  Samples for Composition ( $x=1.0, 1.1, 1.3$  and  $1.4$ ).



**Fig. 9:** Correlation between Degree of Ordering and Saturation Magnetization with Composition  $x$  of  $\text{SrBaFe}_x\text{Mo}_{2-x}\text{O}_6$  Samples for Composition ( $x=1.0, 1.1, 1.3$  and  $1.4$ ).

## CONCLUSIONS

It is reported here that  $\text{SrBaFe}_x\text{Mo}_{2-x}\text{O}_6$  ( $x=1.0, 1.1, 1.3$  and  $1.4$ ) compound prepared by sonochemical method is in a single phase with cubic structure and lattice parameters were found to vary with Fe composition  $x$ . Average grain size of compound was confirmed from SEM pictures. Purity and elements present in final compound were investigated using EDS technique. Perovskite structure formation is confirmed from FTIR spectra. Magnetic properties of all samples in compound were investigated using VSM technique and from M-H loop  $M_s$ ,  $M_r$  and  $H_c$  were evaluated. Saturation magnetization was clearly varying with Fe composition  $x$  and which is in correlation with degree of Fe/Mo ordering.

## ACKNOWLEDGEMENTS

One of the authors (SVP) wishes to thank Principal and HOD dept. of Physics of JNTUACEP for providing lab facility for synthesis. Author (SVP) expresses gratitude to Prof. G. Bhikshamaiah, Dept of Physics, Osmania University for providing gas treatment facility. Author (SVP) thanks Shri

M. Shiva Kumar (IITK), Dr. K. Nageswara Rao (Director P&R, DRDL) for their technical inputs and unconditional support.

## REFERENCES

- Retuerto M, Martinex-Lope MJ, Garcia-Hernandez M, Alonso J A, High-pressure synthesis of the double perovskite  $\text{Sr}_2\text{FeMoO}_6$ : increment of the cationic ordering and enhanced magnetic properties. *J Phys: Condens Matter*. 2009; 21: 186003p.
- Moritomo Y, Xu S, Machida A Akimoto T., Nishibori E., Takata M., Sakata M., Electronic structure of double-perovskite transition-metal oxides. *Phys Rev B*. 2000; 61: R7827p.
- Yang CW, Fang TT. Structures and Development Mechanism of the Anti-Phase Boundaries in  $\text{Sr}_2\text{FeMoO}_6$ . *J Electrochem Soc*. 2012; 159: 35p.
- Kobayashi K.I., Kimura T., Sawada H, Terakura K., Tokura Y. Room-temperature magnetoresistance in an oxide material with an ordered double-perovskite structure. *Nature*. 1998; 395: 677p.

5. Garcia-Landa B, Ritter C, Ibarra MR, Blasco J., Algarabel P.A., Mahendiran R., Garcia J. Magnetic and magnetotransport properties of the ordered perovskite  $\text{Sr}_2\text{FeMoO}_6$ . *Solid State Commun.* 1999; 110: 435p.
6. Maignan A., Raveau B., Martin C., Hervieu M.J., Large Intragrain Magnetoresistance above Room Temperature in the Double Perovskite  $\text{Ba}_2\text{FeMoO}_6$ . *Solid State Chem.* 1999; 144: 224p.
7. Kobayashi KI, Kimura T, Tommioka Y, Sawada H., Terakura K., Tokura Y. Intergrain tunneling magnetoresistance in polycrystals of the ordered double perovskite  $\text{Sr}_2\text{FeReO}_6$ . *Phys Rev B.* 1999; 59: 1159p.
8. Kim TH, Uehara M, Cheong SW, Lee S., Large room-temperature intergrain magnetoresistance in double perovskite  $\text{SrFe}_{1-x}(\text{MoorRe})_x\text{O}_3$ . *Appl Phys Lett.* 1999; 74: 1737p.
9. Aldica G, Plapcianu C, Badica P, Valsangiacom C., Stoica L., Synthesis by oxalic (citric) route and electrical and magnetic characterization of  $\text{Sr}_2\text{FeMoO}_6$  perovskite. *J Mag Mag Mat.* 2007; 311: 665p.
10. Valsangiacom C, Plapcianu C, Stoica L, Aldica G., Kumcser V., Peculiar structural effect of  $\text{Sr}_2\text{FeMoO}_6$  perovskite type compounds. *J of Opto and Adv Mat.* 2008; 10: 845p.
11. Alonso JL, Fernandez LA, Guinea F., Lesmes F., and Martin-Mayor V., Phase diagram and influence of defects in the double perovskites. *Phy Rev B.* 2003; 67: 214423p.
12. Liu GY, Rao GH, Feng XM, Yang H.F., Ouyang Z.W., Liu W.F., Liang J.K., Structural transition and atomic ordering in the non-stoichiometric double perovskite  $\text{Sr}_2\text{FexMo}_2\text{-xO}_6$ . *J Alloy Compd.* 2003; 353: 42–47p.
13. Liu G.Y, Rao G.H., Feng, Z.W. Ouyang, W.F. Liu, J.K. Liang. Metal-semiconductor transition in non-stoichiometry double perovskite  $\text{Sr}_2\text{FexMo}_2\text{-xO}_6$ . *Phys B.* 2003; 334: 229–233p.
14. Markandeya Y., Suresh K., Bhikshamaiah G. Strong correlation between structural, magnetic and transport properties of non-stoichiometric  $\text{Sr}_2\text{FexMo}_2\text{-xO}_6$  ( $0.8 \leq x \leq 1.5$ ) double perovskites. *J Alloys Compd.* 2011; 509: 9598–9603p.
15. Liang Pei, Jiang Jian-Jun, Xin-Guo MA, Xin-guo, Tian Bin. *Trans Nonferrous Met Soc China.* 2007; 17: 109p.
16. Liu Xiao-Jun, Huang Qiao-Jian, Niu Dong-Lin, X U Sheng, Zhang Shu-Yi, Chin. Thermal Diffusivity of Ordered Double Perovskite  $\text{A}_2\text{FeMoO}_6$  (A = Ca, Sr and Ba). *Chin Phys Lett.* 2004; 21: 2281p.
17. Tatsuo Goko, Yoshiyuki Endo, Eiji Morimoto, Juichiro Arai, Takehiko Matsumoto, Pressure effect on transport and magnetic properties of  $\text{A}_2\text{FeMoO}_6$  (A= Ba, Sr). *Physica B.* 2003; 329–333: 837–839p.
18. Liang J.K., Structural transition and atomic ordering in the non-stoichiometric double perovskite  $\text{Sr}_2\text{FexMo}_2\text{-xO}_6$ . *J Alloy Compd.* 2003; 353: 42–47p.
19. Liu G.Y, Rao G.H., Feng X.M., Yang H.F., Ouyang Z.W., Liu W.F., Liu G.Y., Rao G.H., Feng X.M., Ouyang Z.W., Liu W.F., Liang J.K. Metal-semiconductor transition in non-stoichiometry double perovskite  $\text{Sr}_2\text{FexMo}_2\text{-xO}_6$ . *Phys B.* 2003; 334: 229–233p.
20. Markandeya Y., Suresh K., Bhikshamaiah G. Strong correlation between structural, magnetic and transport properties of non-stoichiometric  $\text{Sr}_2\text{FexMo}_2\text{-xO}_6$  ( $0.8 \leq x \leq 1.5$ ) double perovskites. *J Alloys Compd.* 2011; 509: 9598–9603p.
21. Dinesh Topwal, Sarma D.D, Kato H., Tokura Y., Avignon M. Structural and magnetic properties of  $\text{Sr}_2\text{Fe}_{1+x}\text{Mo}_{1-x}\text{O}_6$  ( $-1 \leq x \leq 0.25$ ). *Phys Rev B.* 2006; 73: 094419p.
22. Minfeng Lu, Junjie Li, Xiafeng Hao, Zheng Yang, Defeng Zhou, Jian Meng. Hole doping double perovskites  $\text{Sr}_2\text{FeMo}_{1-x}\text{O}_6$  ( $x = 0, 0.03, 0.04, 0.06$ ) and their Mössbauer, crystal structure and magnetic properties. *J Phys: Condens Mat.* 2008; 20: 175213p.
23. Moghtada, R. Ashiri. Superiority of sonochemical processing method for the synthesis of barium titanate nanocrystals in contrast to the mechanochemical approach. *Ultrason Sonochem.* 2018; 41: 127p.

24. Thitirat Charoonsuk, Wanwilai Vittayakorn, Naratip Vittayakorn, Panpailin Seeharaj, Santi Maensiri. Sonochemical synthesis of monodispersed perovskite barium zirconate ( $\text{BaZrO}_3$ ) by using an ethanol-water mixed solvent. *Ceram Int.* 2015; 41: 87p.
25. Abdolmajid Moghtada, Rouholah Ashiri. Enhancing the formation of tetragonal phase in perovskite nanocrystals using an ultrasound assisted wet chemical method. *Ultrason Sonochem.* 2016; 33: 141p.
26. Dimple P. Dutta, A.K. Tyagi. Weak room temperature ferromagnetism and ferroelectric behavior in sonochemically synthesized bismuth and iron codoped  $\text{SrTiO}_3$  nanoparticles. *Mater Lett.* 2016; 164: 368p.
27. Abdolmajid Moghtada, Ali Shahrouzianfar, Rouholah Ashiri. Low-temperature ultrasound synthesis of nanocrystals  $\text{CoTiO}_3$  without a calcination step: Effect of ultrasonic waves on formation of the crystal growth mechanism. *Adv Powder Technol.* 2017; 28: 1109p.
28. Songkot Utara, Sitchai Hunpratub. Ultrasonic assisted synthesis of  $\text{BaTiO}_3$  nanoparticles at 25 °C and atmospheric pressure. *Ultrason Sonochem.* 2018; 41: 441p.
29. Jin Ho Bang, Kenneth S. Suslick. Sonochemical synthesis of Nanomaterials. *Chem Soc Rev.* 2013; 42: 2555–2567p.
30. Rezlesu N., Rezlesu E., Dor oftei C., Popa P.D., Ignat M., Digest. *Dig J Nanomater Bios.* 2013; 8: 581–587p.
31. Vibhav pandey, Vivek Verma, R. P. Aloysius, G.L. Bhalla, V.P.S Awana, H. Kishan, R.K. Kotnala, Magnetic and magneto-transport properties of double perovskite  $\text{Ba}_{2-x}\text{Sr}_x\text{FeMoO}_6$  system. *J Mag Mag Mater.* 2009; 321: 2239–2244p.
32. Je Hoon Kim, Geun Young Ahn, Seung-Iel ParK, Chul Sung Kim, Effects of Cr doping on magnetic properties of ordered  $\text{Sr}_2\text{FeMoO}_6$ . *J. Magn. Magn. Mater.* 2004; 282 :295p.
33. Feng X. M., Rao G. H., Liu G. Y., Yang H. F., Liu W. F., Ouyang Z.W., Liang J.K., Effects of Cr doping on the cationic ordering and magnetic properties of  $\text{Sr}_2(\text{Fe}_{1-x}\text{Cr}_x)\text{MoO}_6$ . *Phy B.* 2004; 344: 21–26p.
34. Vegard, L. Die Konstitution der Mischkristalle und die Raumfüllung der Atome. *Zeitschrift für Physik.* 1921; 5: 17p.
35. Mostafa M. F., Ata-Allah S. S., Youssef A.A.A., Refai H.S., Electric and AC magnetic investigation of the manganites  $\text{La}_{0.7}\text{Ca}_{0.3}\text{Mn}_{0.96}\text{In}_{0.04x}\text{Al}_{(1-x)0.04}\text{O}_3$ ; ( $0.0 \leq x \leq 1.0$ ). *J Magn Magn Mater.* 2008; 320; 344p.
36. Lavat A. E., Baran E. J., IR-spectroscopic characterization of  $\text{A}_2\text{BB}'\text{O}_6$  perovskites. *Vib Spectrosc.* 2003; 32(2): 167p.
37. Zhang Q., Rao G.H, Dong H.Z., Xiao Y.G., Feng X.M., Liu G.Y., Zhang Y., Liang J.K. Structural, magnetic and transport properties of double perovskite compounds  $(\text{Sr}_{2-3x}\text{La}_2\text{xBa}_x)\text{FeMoO}_6$ . *Physica B.* 2005; 370: 228–235p.
38. Markandeya Y., Saritha D., Vithal M., Singh A.K., Bhikshamaiah G. Effect of indium doping on structural, magnetic and transport properties of ordered  $\text{Sr}_2\text{FeMoO}_6$  double perovskite. *J Alloys Compd.* 2011; 509: 5195–5199p.
39. Ogale A.S., Ogale S.B., Ramesh R., Venkatesan T., Octahedral cation site disorder effects on magnetization in double-perovskite  $\text{Sr}_2\text{FeMoO}_6$ : Monte Carlo simulation study. *Appl Phys Lett.* 1999; 75: 537p.

**Cite this Article**

Varaprasad S, Thyagarajan K. Sonochemical Synthesis of  $\text{SrBaFe}_x\text{Mo}_{2-x}\text{O}_6$  ( $x=1.0, 1.1, 1.3$  and  $1.4$ ) Double Perovskites: Characterization and Magnetic Properties. *Research & Reviews: Journal of Physics.* 2018; 7(2): 8–17p.